Dual-emissive Iridium(III) Complexes as Phosphorescent Probes with Orthogonal Responses to Analyte Binding and Oxygen Quenching

Zhu, Rongji; Dai, Peiling; Yang, Jun; Zhou, Jie; Zhang, Jin; Zhang, Kenneth Yin; Li, Yonghua; Liu, Shujuan; Lo, Kenneth Kam-Wing; Zhao, Qiang

Published in:
Angewandte Chemie - International Edition

Published: 11/09/2023

Document Version:
Post-print, also known as Accepted Author Manuscript, Peer-reviewed or Author Final version

Published version (DOI):
10.1002/anie.202309178

Publication details:
Zhu, R., Dai, P., Yang, J., Zhou, J., Zhang, J., Zhang, K. Y., Li, Y., Liu, S., Lo, K. K.-W., & Zhao, Q. (2023). Dual-emissive Iridium(III) Complexes as Phosphorescent Probes with Orthogonal Responses to Analyte Binding and Oxygen Quenching. *Angewandte Chemie - International Edition*, *62*(37), Article e202309178. https://doi.org/10.1002/anie.202309178

Dual-emissive Iridium(III) Complexes as Phosphorescent Probes with Orthogonal Responses to Analyte Binding and Oxygen Quenching

Rongji Zhu[a],+ Peiling Dai[a],+ Jun Yang[a],+ Jie Zhou[a], Jin Zhang[a], Kenneth Yin Zhang[a],* Yonghua Li[a],* Shujuan Liu[a], Kenneth Kam-Wing Lo[b], and Qiang Zhao[a][c]*

[a] Mr. R. J. Zhu+, Mrs. P. L. Dai+, Mr. J. Yang+, Mrs. J. Zhou, Mrs. J. Zhang, Prof. K. Y. Zhang, Prof. Y. H. Li, Prof. S. J. Liu and Prof. Q. Zhao,
State Key Laboratory of Organic Electronics and Information Displays & Jiangsu Key Laboratory for Biosensors, Institute of Advanced Materials (IAM)
Nanjing University of Posts and Telecommunications
Nanjing 210023 China
E-mail: iamyzhang@njupt.edu.cn, iamyhli@njupt.edu.cn and iamqzhao@njupt.edu.cn

[b] Prof. K. K.-W. Lo,
Department of Chemistry
City University of Hong Kong
Hong Kong China

[c] Prof. Q. Zhao,
College of Electronic and Optical Engineering & College of Flexible Electronics (Future Technology), Jiangsu Province Engineering Research Center for Fabrication and Application of Special Optical Fiber Materials and Devices
Nanjing University of Posts and Telecommunications
Nanjing 210023 China

[+] These authors contributed equally to this work.

Abstract: Phosphorescent probes often show sensitive response toward analytes at a specific wavelength. However, oxygen quenching usually occurs at the same wavelength and thus hinders the accurate detection of analytes. In this study, we have developed dual-emissive iridium(III) complexes that exhibit phosphorescence responses to copper(II) ions at a wavelength distinct from that where oxygen quenching occurs. The complexes displayed colorimetric phosphorescence response in aqueous solutions under different copper(II) and oxygen conditions. In cellular imaging, variation in oxygen concentration over a large range from 5% to 80% can modulate the intensity and lifetime of green phosphorescence without affecting the response of red phosphorescence toward intracellular copper(II) ions.

Cationic phosphorescent iridium(III) polypyridine complexes of the general structural formula $[Ir(N^C)_2(N^N)]^+$, where N^C is a cyclometalating ligand and N^N is a diimine ligand, have gained tremendous attention as biological probes and cellular imaging reagents.[1–3] The complexes are attractive for their long-lived phosphorescence, sensitive excited-state properties, efficient cellular uptake, and the tunable ability to target organelles.[4–6] Depending on the energy levels of the frontier molecular orbitals, these complexes typically exhibit a triplet intraligand (^{3}IL) or metal-/ligand-to-ligand charge transfer (^{3}MLCT/^{3}LLCT) emissive state.[7–9] As biological probes, these complexes display phosphorescence changes in intensity and lifetime when exposed to specific substances or changes in environmental parameters, while the spectral profile and characteristics remain mostly unchanged.[10,11]

Recently, dual-emissive iridium(III) complexes have emerged as new functional tools in biotechnology.[12–16] These complexes emit light at two different wavelengths with sensitive emission profiles, thus providing several advantages over single-wavelength emitting complexes as biological probes. Firstly, they show wavelength-ratiometric response, avoiding interference from concentration or excitation-induced intensity fluctuations. Secondly, their spectral response is always accompanied by an observable change in luminescence color, which is easily distinguishable to the naked eye. Thirdly, they emit light from two independent excited states, theoretically enabling simultaneous responses toward two analytes, although this attractive property has not been demonstrated yet. Fourthly, phosphorescent complexes can be quenched by oxygen molecules,[17,18] and intensity or lifetime response toward a specific analyte may be interfered if the oxygen distribution is uneven, as is likely in biological environments such as living cells. Dual-emissive phosphorescent iridium(III) complexes could potentially be utilized as optimal candidates that are able to respond to analyte binding and oxygen quenching at different wavelengths.

Despite the advantages mentioned above, the progress of dual-emissive molecular probes was slow due to a lack of a general design strategy. A charge-neutral dual-emissive iridium(III) complex has been reported as ratiometric sensor for copper(II) ion, but its poor cellular uptake limited the application in live cell imaging.[19] We have previously found that positively-charged cyclometalated iridium(III) polypyridine complexes with unconjugated amino groups were potential dually emissive and used them as ratiometric probes for various proteins[20,21] and molecular oxygen.[22] In the current work, we incorporated di(2-picolyl)-amine (DPA) as a copper(II) binding site[23–25] into the dual-emissive skeleton, developing two novel dual-emissive complexes **1** and **2** (Figure 1a). A single-wavelength emissive complex **3** without the unconjugated amino groups in the cyclometalating ligands was also synthesized for comparison study. The synthesis and characterization data of the complexes were provided in the Supporting Information. All the complexes were

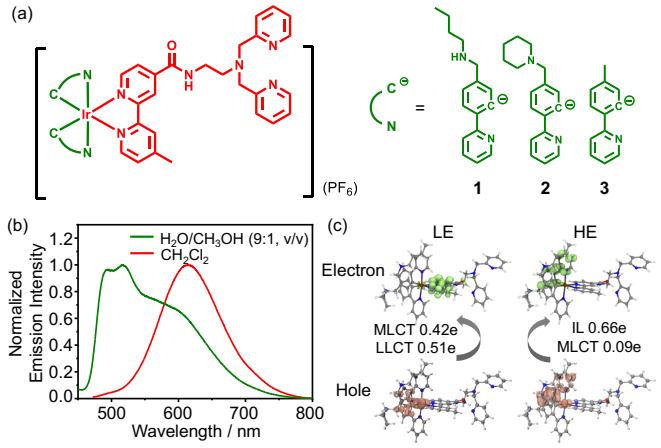

Figure 1. (a) Chemical structures of complexes **1** – **3**. (b) Normalized emission spectra of complex **1** in deaerated CH_2Cl_2 and H_2O/CH_3OH (9:1, v/v) at 298 K under excitation at 365 nm. (c) Isosurface plots (isovalue = 0.0030) of electron-hole distributions and transferred electron in the HE and LE emissive states of complex **1** in water.

characterized by ^1H and ^{13}C nuclear magnetic resonance (NMR) spectroscopy, positive-ion matrix-assisted laser desorption ionization time-of-flight (MALDI TOF) mass spectrometry (MS), and ultraviolet-visible (UV-Vis) absorption spectroscopy. The NMR and MS spectra of the diamine ligand and the dual-emissive complexes **1** and **2** are shown in Figure S1 – S11. The electronic absorption spectra of the complexes are shown in Figure S12, and the spectral data are listed in Table S1.

Upon irradiation, all the complexes displayed long-lived phosphorescence in the visible region. The photophysical data of the complexes in deaerated solvents at room temperature are summarized in Table S2. The emission spectra of complex **1** in CH_2Cl_2 and aqueous solution are illustrated in Figure 1b and those of complexes **2** and **3** are shown in Figure S13. While complex **3** showed a broad emission band at 590 – 617 nm, complexes **1** and **2** containing the amino groups featured high-energy (HE) green and low-energy (LE) red dual emission at 493 – 520 nm and 598 – 615 nm, respectively, in fluid solutions at room temperature. In less polar CH_2Cl_2, the LE emission band of complexes **1** and **2** was dominant, with the HE bands completely embedded (Table S2). In CH_3CN, the HE emission of complexes **1** and **2** appeared as a shoulder. In polar aqueous solution, the HE band was predominant, and the LE band became a shoulder. Although the HE and LE bands significantly overlapped in wavelength, they are well resolved in the time scale. The lifetimes of the HE green emission (τ_0 = 1.5 – 4.1 μs) were much longer than those of the LE red emission (τ_0 = 78 – 227 ns). The large Stokes shifts and long lifetimes indicate triplet-state nature of both the HE and LE emission. They are assigned to ^{3}IL $\pi \rightarrow \pi^*$ (N^C) and ^{3}MLCT/^{3}LLCT $d\pi(Ir)/\pi(N^C) \rightarrow \pi^*(N^N)$ excited states, respectively. The assignment was supported by the observations that the emission from the charge transfer (^{3}CT) excited state showed reduced emission lifetimes and quantum yields upon increasing solvent polarity, whereas the emission from the ^{3}IL state was less affected by the solvent and became dominant in polar solvents.[20–22]

To investigate the transition features of the two emissive states, theoretical computational studies were performed using time-dependent density functional theory (TD-DFT).[26] The electronic excitation process of both emissive states was examined through inter-fragment charge transfer (IFCT) using the Multiwfn program.[27] The electron and hole distributions[28] in the HE and LE emissive states of complex **1** were shown in Figure 1c. In the LE state, the iridium(III) center and the C^N ligand donate 0.42 and 0.51 electron, respectively, to the N^N ligand, indicating a charge-transfer state involving a total of 0.93 electron. In the HE state, there is an IL transition involving 0.66 electron and an MLCT transition involving 0.09 electron towards the C^N ligand. Similar conclusion was obtained through natural transition orbital (NTO) analysis.[29] The LE state primarily involves a charge transfer transition from the iridium(III) center and the C^N ligand to the N^N ligand, whereas the HE state is predominantly relies on the IL transition occurring on the C^N ligands (Figure S14). Similar transitions were also observed for complex **2** (Figure S15).

The emission responses of the complexes toward oxygen and copper(II) ions were investigated. The emission spectra of complex **1** (10 μM) under N_2, air, and O_2 atmosphere in the absence and presence of $CuCl_2$ (10 μM) in an aqueous solution are shown in Figure 2a. Complex **2** exhibited similar properties to complex **1**, and related spectra are shown in Figure S16. Interestingly, while the dual-emissive complexes **1** and **2** displayed preferential quenching of the HE green emission with increasing environmental oxygen concentration, copper(II) binding selectively quenches the LE red emission. The complexes exhibited

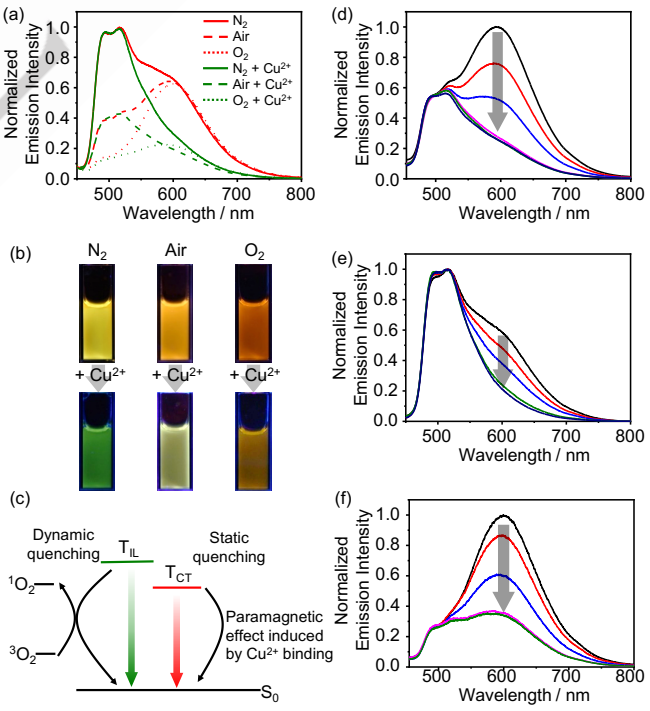

Figure 2. (a) Emission spectra of complex **1** (10 μM) in N_2 (solid line), air (dashed line) and O_2 (dotted line) saturated H_2O/CH_3OH (9:1, v/v) in the absence (red) and presence (green) of $CuCl_2$ (10 μM) and (b) the corresponding photographs. (c) Energy diagrams illustrating the quenching processes. (d–f) Emission spectral traces of complex **1** (10 μM) in air (d), N_2 (e) and O_2 (f) saturated H_2O/CH_3OH (9:1, v/v) upon addition of 0 – 10 μM $CuCl_2$.

significant changes in emission color under different oxygen and copper(II) ion conditions (Figure 2b and S17). In sharp contrast, the single-wavelength emitting complex **3** underwent similar emission quenching at the same wavelength under either increasing oxygen concentration or copper(II) binding (Figure S18), with its emission maximum and color remaining unchanged under various conditions.

To further investigate the quenching processes of the dual-emissive complexes **1** and **2**, lifetime measurements were conducted. With increasing oxygen concentration from 0 to 100%, the HE emission lifetime of complexes **1** and **2** at around 490 nm decreased from 4.0 to 0.18 μs and from 4.1 to 0.21 μs, respectively, in aqueous solution, indicating a dynamic collision deactivation quenching process (Figure 2c). The Stern-Volmer constants (K_{sv}) for complexes **1** and **2** were calculated as about $0.30\%^{-1}$ and $0.29\%^{-1}$, respectively, based on the HE emission lifetime values (Figure S19). Meanwhile, the LE emission lifetimes of the complexes at 620 nm were slightly reduced from 86 and 78 ns to 75 and 59 ns, respectively ($K_{sv} < 0.01\%^{-1}$). The preferential oxygen quenching of the HE emission was due to the much longer excited-state lifetime than that of the LE emission, providing a greater opportunity to interact with nearby oxygen molecules before emitting photons.

The copper(II) binding induced quenching was investigated via emission titrations using $CuCl_2$ as the titrant. The emission spectral traces of complexes **1** and **2** upon addition of $CuCl_2$ in aqueous solutions are shown in Figures 2d and S20. Selective quenching of the LE emission was observed while the HE emission intensity remained almost unchanged. The HE and LE emission lifetimes at 490 and 620 nm fluctuated in the ranges of 0.75 – 0.79 μs and 64 – 80 ns, respectively, indicating that selective quenching of the LE emission by copper(II) is a static process (Figure 2c) resulting from the formation of DPA-Cu^{2+} adducts with the paramagnetic Cu^{2+} ion.[30] The copper(II) binding and resultant emission response were reversible. The LE emission recovered to almost the original intensity upon addition of 100 equivalent of the metal-chelating agent EDTA disodium (Figure S21). The emission response was selective toward Cu^{2+}

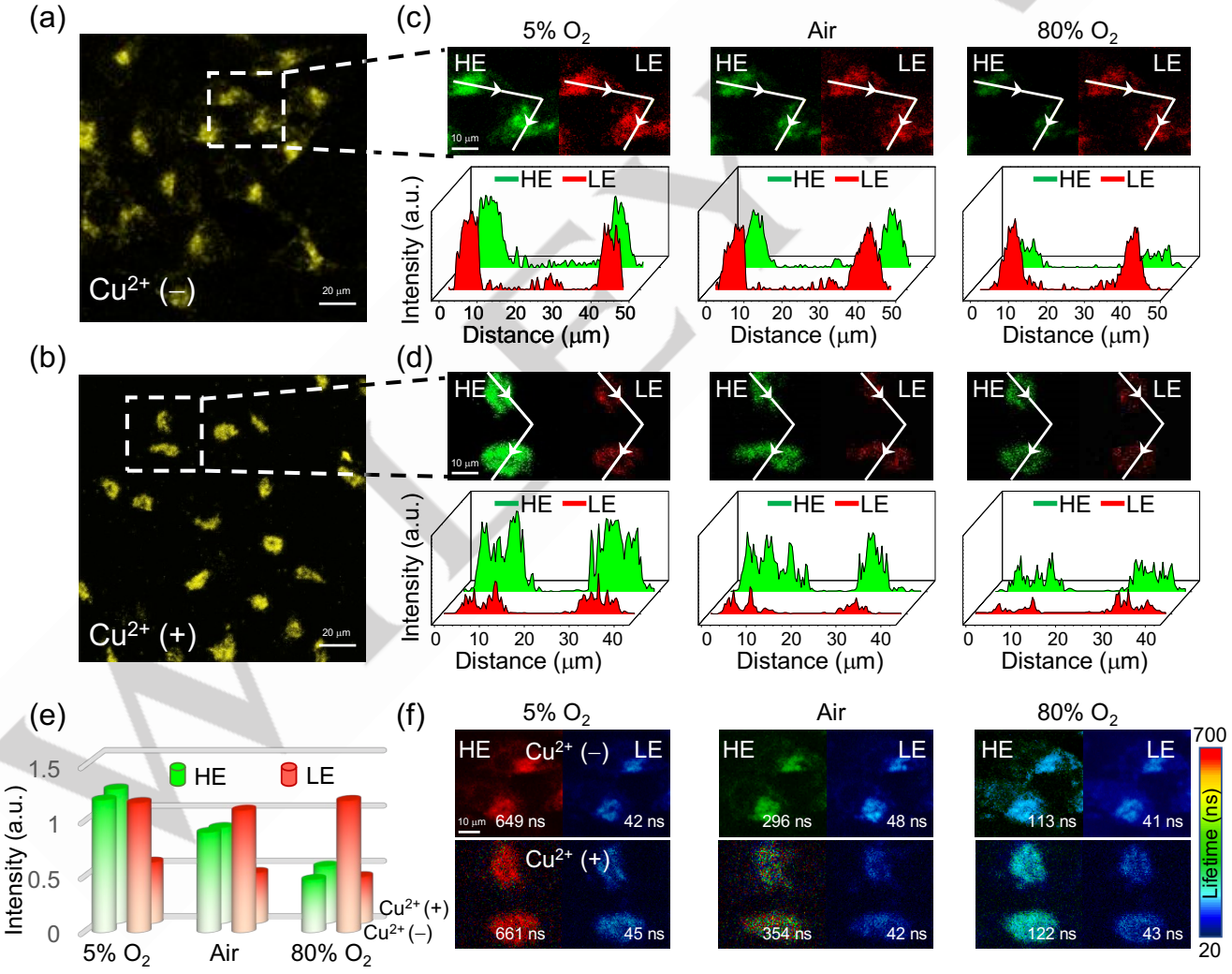

Figure 3. (a,b) LSCM images of HeLa cells incubted with complex **1** (15 μM, 2 h) before (a) and after (b) treatment with $CuCl_2$ (100 μM, 1 h). λ_{em} = 500 – 650 nm. (c,d) LSCM images and dual emission intensity analysis cross complex **1**-loaded HeLa cells without (c) and with (d) treatment with $CuCl_2$ (100 μM, 1 h) and further incubated under different oxygen concentrations for 30 min. λ_{HE} = 500 – 550 nm; λ_{LE} = 600 – 650 nm. (e,f) Relative emission intensity (e) and PLIM images with averaged lifetime values (f) HeLa cells incubted with complex **1** (15 μM, 2 h) without and with treatment with $CuCl_2$ (100 μM, 1 h) and further incubated under different oxygen concentrations for 30 min.

over other common biological relevant metal ions including Al^{3+}, Ca^{2+}, Co^{2+}, K^{+}, Li^{+}, Mn^{2+}, Na^{+}, Ni^{2+}, Zn^{2+} (Figure S22), and unaffected by pH values over a wide range of 3.0 – 8.0 (Figure S23). The equivalence points of the titrations occurred at [Ir]:[Cu^{2+}] = about 0.56 and 0.52 for complexes **1** and **2**, respectively. Furthermore, the emission titrations were also performed under pure N_2 and O_2 atmospheres and the spectral traces are shown in Figure 2e and 2f. Notably, the oxygen concentration in the surroundings affected the intensity of the HE emission, either increasing or decreasing it, but did not interfere the response of the LE emission to copper(II) ions. The detection limits were found to be similar under different conditions, ranging from 0.19 to 0.51 μM.

The complexes were utilized for cellular imaging through laser-scanning confocal microscopy (LSCM) and photoluminescence lifetime imaging microscopy (PLIM). The 3-(4,5-dimethyl-2-thiazolyl)-2,5-diphenyltetrazolium bromide (MTT) assay showed that HeLa cells incubated with the complexes at concentrations below 60 μM for 24 h at 37°C maintained good viability (Figure S24). LSCM images revealed that HeLa cells treated with complexes **1** and **2** (15 μM, 2 h) displayed cytoplasmic staining. Costaining experiments involving Lyso-Tracker Red showed that the intracellular complexes were concentrated in the lysosomes (Figure S25). LSCM images of live HeLa cells loaded with complexes **1** and **2** (15 μM, 2 h) under different oxygen and copper(II) ion conditions are shown in Figure 3a–d, S26 and S27. The HE and LE emission was independently analyzed in the green (500 – 550 nm) and red (600 – 650 nm) channels, respectively (Figure 3c–f). In the absence of $CuCl_2$, variation in the oxygen concentration did not significantly affect the LE emission, but the HE emission was stronger under 5% O_2 and became much weaker under 80% O_2 (Figure 3c). Further incubation of the cells with $CuCl_2$ (100 μM, 1 h) led to remarkable LE emission quenching regardless of oxygen concentration (Figure 3d). In the case of LE emission being quenched by copper(II) ions, the HE emission exhibited a similar response to oxygen concentration in the presence of $CuCl_2$ as in its absence. The relative intracellular intensities of the HE and LE emission were illustrated in Figure 3e. It clearly showed that the HE and LE emission sensitively and independently responded to oxygen and copper(II) ions, respectively, without crosstalk. This demonstrated the significant advantage of dual-emissive phosphorescent complexes as biological probes, where the response of phosphorescence to the target analyte is not disturbed by oxygen quenching. The PLIM analysis showed that oxygen preferentially quenched the HE emission lifetimes whereas copper(II) ions had negligible effect on both HE and LE emission lifetimes (Figure 3f). This is consistent with the fact that the emission quenching by oxygen and copper(II) ions were dominantly dynamic and static processes, respectively.

In conclusion, we have proposed a universal design approach for developing dual-emissive phosphorescent biological probes through incorporation of an analyte-recognition site into the dual-emissive iridium(III) skeleton structures. The probes exhibited longer-lived HE and relatively shorter-lived LE phosphorescence. Oxygen quenching preferentially occurred at HE emission while analyte-binding selectively induced LE emission response. To the best of our knowledge, this is the first example that a molecular phosphorescent probe that is responsive toward oxygen quenching and analyte binding at two different wavelengths. This finding provides new insights into the understanding of phosphorescent probes and helps us to better design and optimize the sensing behavior. Furthermore, the distinct response characteristics also provide new ideas for developing novel sensors.

Acknowledgements

This work was supported by National Natural Science Foundation of China (61975085, 22075148, 22161160318) and National Natural Science Foundation of China and Hong Kong Research Grants Council (Project No. N_CityU104/21) for financial support. K.Y.Z. acknowledges the receipt of Qing Lan Project of Jiangsu Province.

Conflict of Interest

The authors declare no conflict of interest.

Data Availability Statement

The data that support the findings of the study are available in the supplementary material of this article.

Keywords: bioimaging • dual-emission • iridium • phosphorescence • probes

[1] P.-Y. Ho, C.-L, Ho, W.-Y. Wong, *Coord. Chem. Rev.* **2020**, *413*, 213267.
[2] X. H. Tian, C. D. Pace, L. Ruiz-Perez, B. Chen, R. Su, M. Z. Zhang, R. L. Zhang, Q. Zhang, Q, Wang, H. P. Zhou, J. Y. Wu. Z. P. Zhang, Y. P. Zhang, Y. P. Tian, G. Battaglia, *Adv. Mater.* **2020**, *32*, 2003901.
[3] L. C.-C. Lee, K. K.-W. Lo, *J. Am. Chem. Soc.* **2022**, *144*, 14420–14440.
[4] K. K.-W. Lo, *Acc. Chem. Res.* **2020**, *53*, 32–44.
[5] C. Caporale, M. Massi, *Coord. Chem. Rev.* **2018**, *363*, 71–91.
[6] B. H. Jhun, D. Song, S. Y. Park, Y. You, *Top. Curr. Chem.* **2022**, *380*, 35.
[7] H. Amouri, *Chem. Rev.* **2023**, *123*, 230–270.
[8] P. Tao, X. Lü, G. Zhou, W.-Y. Wong, *Acc. Mater. Res.* **2022**, *3*, 830–842.
[9] F. Monti, A. Baschieri, L. Sambri, N. Armaroli, *Acc. Chem. Res.* **2021**, *54*, 1492–1505.
[10] K. K.-W. Lo, *Acc. Chem. Res.* **2015**, *48*, 2985–2995.
[11] J. Zhou, J. L. Li, K. Y. Zhang, S. J. Liu, Q. Zhao, *Coord. Chem. Rev.* **2022**, *453*, 214334.
[12] S. Kumar, Y. Hisamatsu, Y. Tamaki, O. Ishitani, S. Aoki, *Inorg. Chem.* **2016**, *55*, 3829–3843.
[13] Y. Hisamatsu, S. Kumar, S. Aoki, *Inorg. Chem.* **2017**, *56*, 886–899.
[14] P. Zhao, S. Tofighi, R. M. O'Donnell, J. M. Shi, M. V. Bondar, D. J. Hagan, E. W. Van Stryland, *J. Phys. Chem. C* **2018**, *122*, 6786–6793.
[15] C. Climent, P. Alam, S. S. Pasha, G. Kaur, A. R. Choudhury, I. R. Laskar, P. Alemany, D. Casanova, *J. Mater. Chem. C* **2017**, *5*, 7784–7798.

[16] A. Y. Gitlina, M. V. Ivonina, V. V. Sizov, G. L. Starova, A. P. Pushkarev, D. Volyniuk, S. P. Tunik, I. O. Koshevoy, E. V. Gra-chova, *Dalton Trans.* **2018**, *47*, 7578–7586.

[17] X. D. Wang, O. S. Wolfbeis, *Chem. Soc. Rev.* **2014**, *43*, 3666–3761.

[18] H. N. Kagalwala, J. Gerberich, C. J. Smith, R. P. Mason, A. R. Lippert, *Angew. Chem. Int. Ed.* **2022**, *61*, e202115704. *Angew. Chem.* **2022**,*134*, e202115704.

[19] Y. You, Y. Han, Y.-M. Lee, S. Y. Park, W. Nam, S. J. Lippard, *J. Am. Chem. Soc.* **2011**, *133*, 11488–11491.

[20] K. K.-W. Lo, K. Y. Zhang, S.-K. Leung, M.-C Tang, *Angew. Chem. Int. Ed.* **2008**, *47*, 2213–2216. *Angew. Chem.* **2008**, *120*, 2245–2248.

[21] K. Y. Zhang, H.-W. Liu, M.-C. Tang, A. W.-T. Choi, N. Zhu, X.-G. Wei, K.-C. Lau, K. K.-W. Lo, *Inorg. Chem.* **2015**, *54*, 6582–6593.

[22] K. Y. Zhang, P. L. Gao, G. L. Sun, T. W. Zhang, X. L. Li, S. J. Liu, Q. Zhao, K. K.-W. Lo, W. Huang, *J. Am. Chem. Soc.* **2018**, *140*, 7827–7834.

[23] Y. Ma, B. Z. Zheng, Y. Zhao, H. Y. Yuan, Y. Q. Cai, J. Du, D. Xiao, *Biosens. Bioelectron.* **2013**, *48*, 138–144.

[24] X. L. Zhang, X. Jing, T. Liu, G. Han, H. Q. Li, C. Y. Dun, *Inorg. Chem.* **2012**, *51*, 2325–2331.

[25] S. Sakunkaewkasem, A. Petdum, W. Panchan, J. Sirirak, A. Char-oenpanich, T. Sooksomuang, N. Wanichacheva, *ACS Sens.* **2018**, *3*, 1016–1023.

[26] E. Runge, E. K. U. Gross, *Phys. Rev. Lett.* **1984**, *52*, 997–1000.

[27] T. Lu, F. Chen, *J. Comput. Chem.* **2012**, *33*, 580–592.

[28] Z. Liu, T. Lu, Q. Chen, *Carbon* **2020**, *165*, 461–467.

[29] R. L. Martin, *J. Chem. Phys.* **2003**, *118*, 4775–4777.

[30] M. Formica, V. Fusi, L. Giorgi, M. Micheloni, *Coord. Chem. Rev.* **2012**, *256*, 170–192.

Entry for the Table of Contents

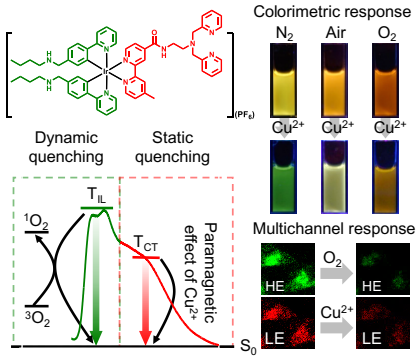

We reported dual-emissive iridium(III) complexes bearing a di(2-picolyl)-amine (DPA) unit, which exhibited green and red dual phosphorescence in aqueous solutions. The complexes exhibited static and dynamic phosphorescence quenching in response to copper(II) ions and oxygen, respectively, at different wavelengths, achieving colorimetric emission response in solutions and multichannel response in live cell imaging.